Experimental Progress in Nulling Interferometry: Comparison of Null Stabilization Approaches

E. Serabyn
Jet Propulsion Laboratory
Mail Stop 171-113
4800 Oak Grove Drive
California Institute of Technology
Pasadena, CA 91109
818-393-5243
gene.serabyn@jpl.nasa.gov

Abstract— Nulling interferometry is a technique which can potentially enable the direct detection of light from planets orbiting around nearby stars. In this approach, the light from two or more telsescopes is combined using achromatic destructive interference so that the incident bright stellar light cancels on the optical axis to high accuracy, thus leaving the radiation from off-axis source more amenable to detection. Deep nulling of broadband thermal white light has now been demonstrated in the laboratory, and two different null-stabilization algorithms have been demonstrated experimentally. In this report, the two null fringe stabilization approaches which have been demonstrated experimentally are compared on a theoretical basis, and laboratory results obtained with both stabilization approaches are presented. Finally, a brief status update on the current performance levels achieved is included.

TABLE OF CONTENTS

1. INTRODUCTION

The presence of planets around nearby stars can be inferred by indirect means, i.e., by observations of stellar parameters affected by the presence of planets, such as stellar Doppler shifts, lateral stellar wobble, and brightness variations due to partial eclipses by transiting planets, or by direct observation of their emitted or reflected light. Although indirect evidence for planets around nearby stars by means of the Doppler technique is accumulating rapidly, and one example of a planetary transit has been observed, direct detection of radiation from such planets still lies in the future. The reason for this lies in the combination of the large brightness contrast ratio between stars and planets, coupled with their close proximity to each other. (At a distance of 10 pc, the Earth would be only 0.1 arc seconds away from the star). The contrast ratio is improved by moving from optical to mid-infrared wavelengths, where planetary emission peaks, but even so, contrast ratios of over 1,000,000:1 can be expected at mid-infrared wavelengths for Earth-like or Jupiter-like planets around nearby stars. Thus to characterize planetary companions to nearby stars, a way of selectively ``dimming" the star relative to it's surroundings is needed.

To overcome this brightness contrast, a number of approaches can be employed. The most obvious is to increase the size of the collecting aperture, so that the size of the telescope's Airy pattern is decreased, but at present the needed aperture diameters are prohibitively large (at least several tens of meters). Thus, it is more profitable to consider approaches in which the intrinsic contrast ratio is adjusted, by selectively rejecting the on-axis starlight. There are at present two ideas on how to go about this. The first is the classical approach of coronagraphy, in which a small opaque disk located in a focal plane image is used to light from the stellar disk. Because this technique is necessarily limited to regions of the focal plane more than a few Airy rings from the axis, this approach can naturally best be applied to the Sun's nearest neighbor stars.

Of course, separated-aperture interferometry can also address such problems, by providing the needed higher angular resolution without the need to employ larger telescope apertures. Even so, the need to reject the bright stellar light remains. In the case of interferometry, the stellar cancellation can be naturally effected by positioning the star at the bottom of a destructive interference fringe. To maximize the effect of this approach, an achromatic dark fringe is needed, so that the starlight can be canceled, or nulled, to deep levels across a wide radiation bandwidth. This approach, called ``nulling interferometry", requires both a high degree of symmetry and stability and a low degree of residual spectral dispersion in the optical beam trains, in order to enable the deep, stable, and

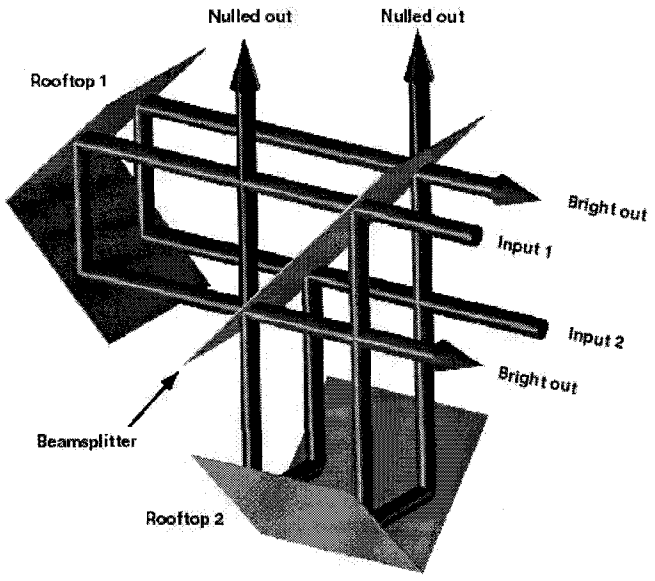

broadband rejection of starlight at the central zero optical path difference (OPD) fringe.

Starlight rejection of order 1,000,000:1 at thermal infrared wavelengths (5-20 microns) can only be achieved if the different optical pathlengths are matched to an accuracy of order 1 nm. In addition, a number of other stringent constraints, on e.g., relative field rotation, field-amplitude matching, polarization equivalence, etc., must be met. Thus, experimental demonstrations of different approaches to nulling interferometry, both in the laboratory and on telescopes, are needed prior to deployment of nulling interferometers on space-based platforms such as e.g., the Space Interferometer Mission (SIM), or the Terrestrial Planet Finder (TPF). A laboratory demonstration of deep and stable nulling has recently been obtained, using an approach in which the incident fields are given a relative field flip inside a beam-combining rotational-shearing interferometer [1], but much development work remains to be done. The intent of this paper is to provide a comparison of the null-fringe stabilization approaches applied to this experiment, and to present an update on the latest experimental results obtained therewith. This paper begins with a brief introduction to nulling beam combiners, in order to set the stage for the following discussion. It then goes on to compare null-fringe stabilization techniques from a theoretical point of view. The final sections provides an update on the most recent nulling results obtained at the Jet Propulsion Laboratory. These results have demonstrated the ability to achieve the full set of performance requirements set for the nulling experiment being considered for inclusion in the Space Interferometer Mission, with the exception of dual-polarization operation.

2. Nulling of Light With A Rotational Shearing Interferometer

The main reason to consider a rotational shearing interferometer as a means of nulling light is that it can be used to introduce a geometric field flip between the two beams to be combined. Since a geometric field flip is an achromatic (wavelength-independent) means of producing the needed field reversal, rotational shearing interferometers can produce simultaneous cancellation of incident starlight over a broad radiation bandwidth. In the approach developed and demonstrated at the Jet Propulsion Laboratory, the field flip is carried out by a pair of orthogonal rooftop mirrors defining the end mirrors in the two arms of a rotational shearing interferometer (Figure 1). Each rooftop mirror flips one component of the incident field (that component orthogonal to the rooftop centerline) so that the net effect of the pair of rooftops is a relative flip of the full electric field vector. A diagram of the full optical layout employed is shown in Figure 2, while a photograqph of the actual experiment is provided in Figure 3.

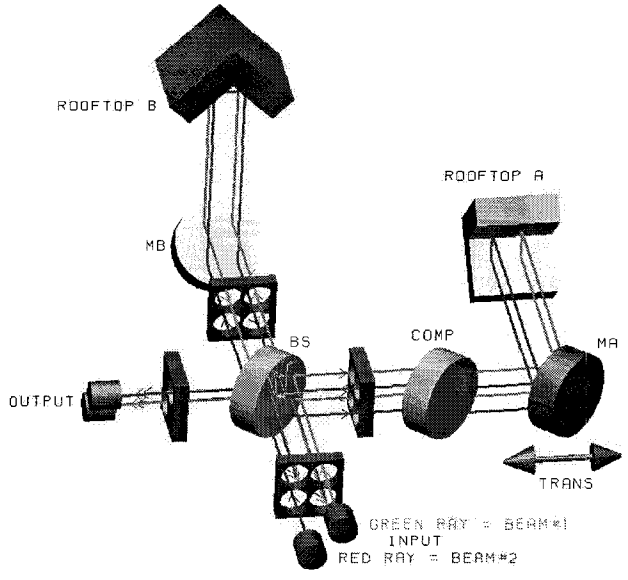

Figure 2. Detailed layout of nulling rotational shearing interferometer, including the fold mirrors needed for polarization compensation.

Other ways to bring about an achromatic field flip exist, one of which is to make use of the field inversion which occurs upon passage through a focus. For the purposes of the ensuing discussion regarding the signal-to-noise tradeoffs between the different null-fringe stabilization approaches to be discussed, the details of the optical implementation are relatively unimportant, and they are not addressed further here.

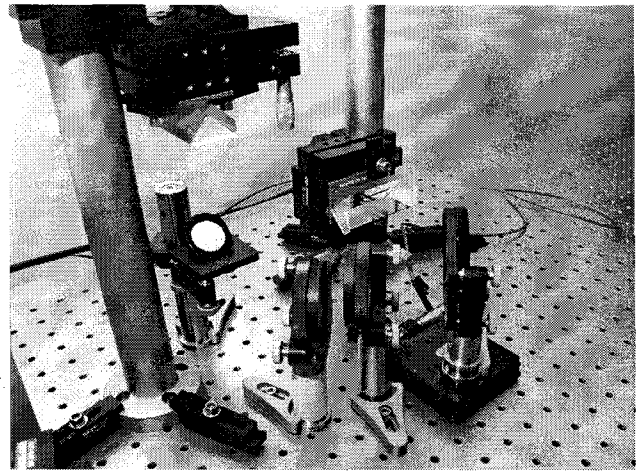

One aspect which is relevant is that in two-port rotational shearing interferometers the two input beams to be combined typically yield four output beams, because of the double-pass beamsplitter arrangement used. In general it is thus possible to arrange two of these outputs to be destructive (nulling) outputs (the ``balanced" outputs which experience one reflection and one transmission at the beamsplitter), whereupon by conservation of energy the other two outputs must be bright (constructive) outputs. Furthermore, by offsetting the two rooftop mirrors and including an additional offset in one of the input beams, it is possible to offset the phases of the outputs as desired [2]. It fact, by making both of the aforementioned optical pathlength offsets equal to an eighth of a wavelength, it is possible to generate a set of four outputs which are equally spaced in phase by $\pi/2$ radians. Of course in the broadband case, only one pair of these outputs (one nulling output and its bright complement) can actually be achromatic, but only the nulling output actually requires achromaticity.

3. Null Fringe Stabilization

To actually detect faint planetary companions to nearby stars, long integrations times will be required, and so the ability to stabilize the interferometer on the null fringe is critical. The first question to consider in terms of null-fringe stabilization schemes is the error signal to be used to determine the current optical path error between the two arms of the interferometer. In general, if both balanced outputs are phased to operate at null, the error signal will be small, as operation at the null fringe implies operation at the bottom of the quadratic (in the small phase error approximation) fringe trough. Thus at null, the slope of the transmitted light leakage term is zero. This situation is actually quite analogous to the case of laser cavity length stabilization, except for the fact that in the latter case, the operating point is located at the top of a fringe instead of at the bottom. However, except for this change in sign of the local curvature of the signal, the actual error signals, which are given by the deviation of the light intensity from the local extremum value, are in principle identical, because the same sinusoid applies. The actual light intensity at the

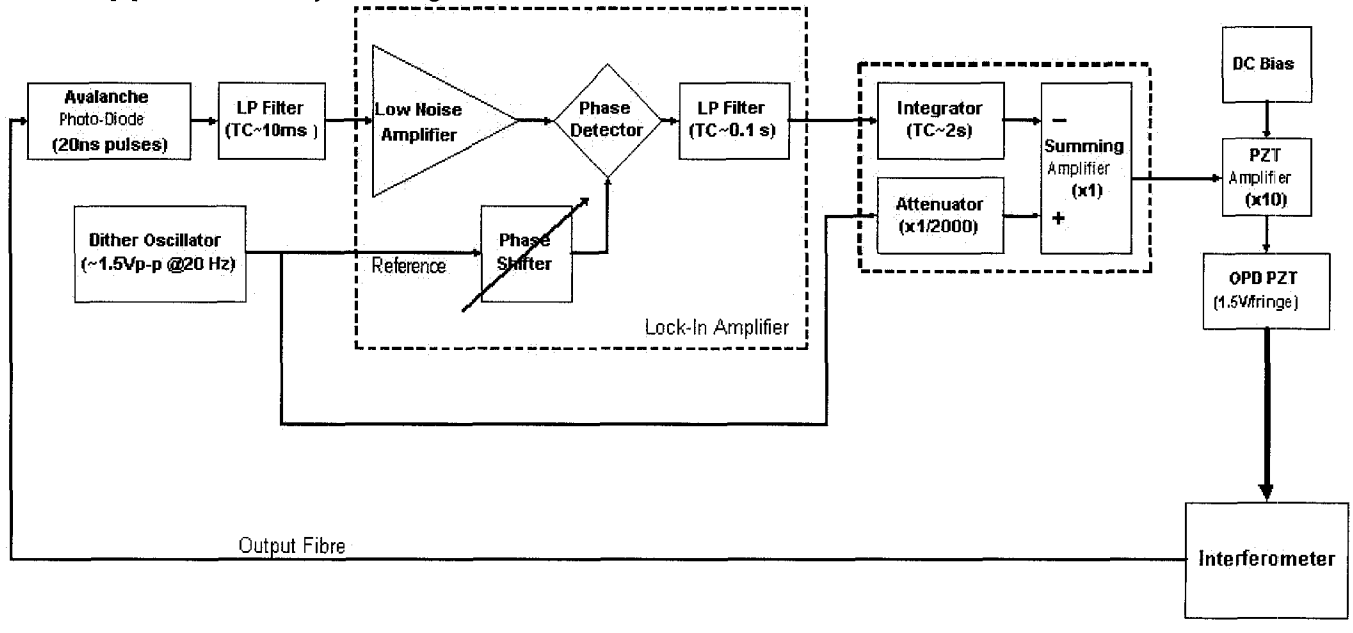

Null Stabilization Loop Block Diagram

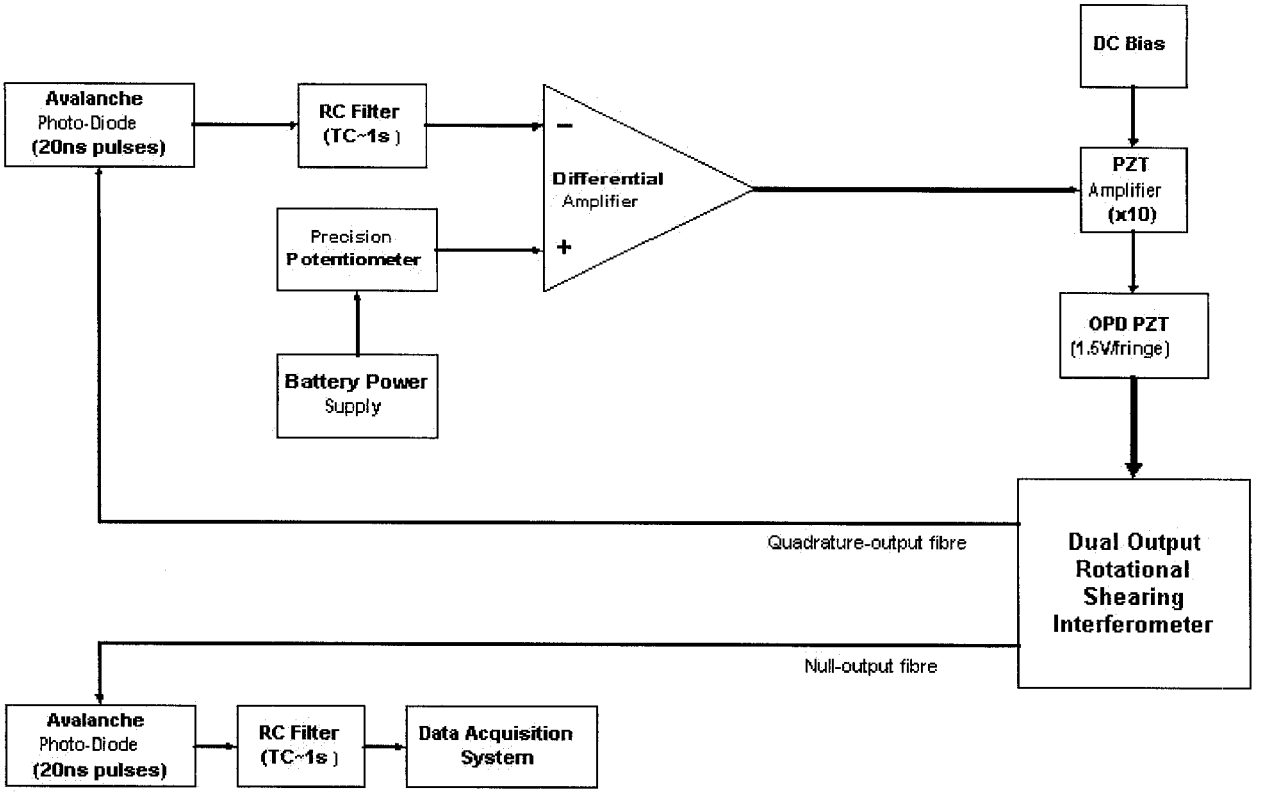

Quadrature-Output Null Stabilization Block Diagram

extremum is then irrelevant. Thus, even with much higher light intensity present at a constructive maximum, the change in flux caused by an error in path length is the same for the constructive and destructive cases.

.

If the positon of a mirror in one arm of the interferometer is dithered sinusoidally in position, the optical path difference will be likewise modulated, resulting in a modulation of the output power. In the case of nulling, the dither amplitude must be kept small enough to keep the light leakage below the acceptable level, meaning a dither of order 1 nm or less. Both the small dither amplitude and the zero slope at the null operating point imply a small error signal in applications dealing with white light, especially in cases where only one spatial mode of a thermal radiation field is under consideration, as it likely will be for nulling to detect planetary companions. Thus it is also important to consider the noise limitation of the dither control approach. Here some initial optimism is warranted, as the low residual light level at null implies a low photon noise level as well.

On the other hand, if one of the two nulling outputs can be sacrificed in order to have it operate instead at the quadrature point, an alternative control algorithm can be considered. Moving to an operating point 90º away in phase means that the operating point of this ``quadrature" output is the zero-crossing point of a sinusoid. Since the slope of the fringe is maximized here, this operating point has the advantage that the error signal for departures from the quadrature operating point is maximized. If the nulling and quadrature outputs are locked to track each other, the control signal for null stabilization is thus maximized. Although this may sounds advantageous initially, again it is important to consider the effects of noise, because although the control signal is larger, so are the photon flux and the photon noise. A detailed signal to noise ratio comparison of the different operating points is therefore called for. This topic is discussed in the next section. For completeness, operation at the fringe minimum, maximum, and derivative maximum are considered.

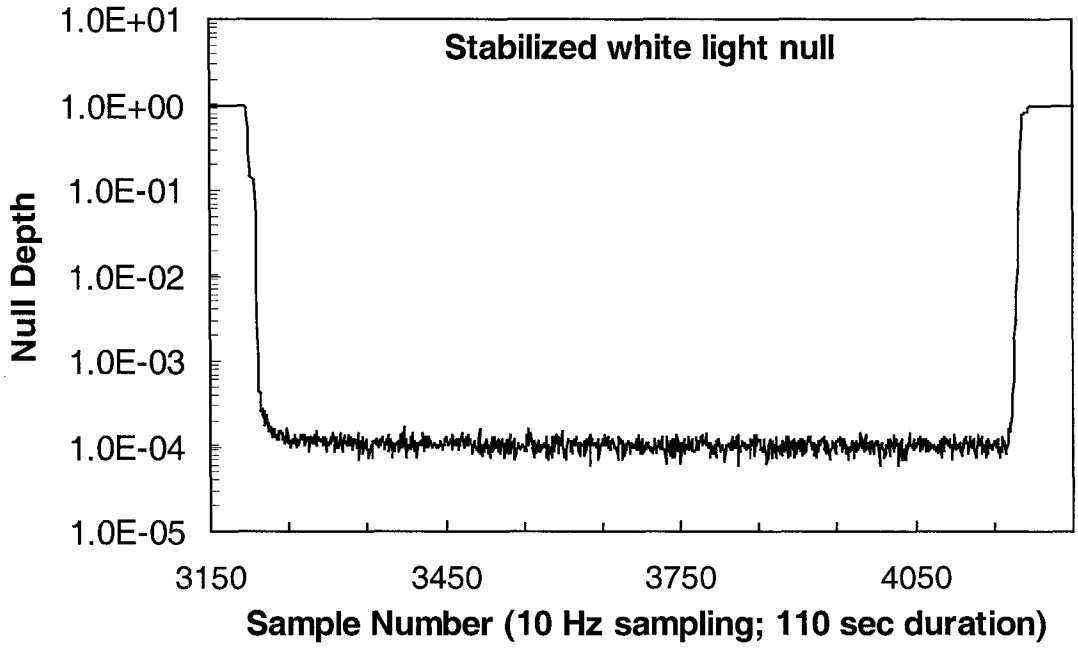

For a perfect monochromatic sinusoidal fringe in an interferometer with a null at zero OPD, the instantaneous light intensity, **I**, arriving at the detector is given as a function of the phase error, ϕ, between the two interferometer arms by

$$I = R[1-\cos(\phi)]/2, \qquad (1)$$

where **R** is the total photon arrival rate at constructive interference (i.e., the sum of the individual aperture fluxes). At null, $\phi = 0$, at quadrature $\phi = \pi/2$, while at the constructive peak $\phi = \pi$. For simplicity, we consider here the monochromatic case.

Near the null position, light leakage from a variety of error sources dominates [3], implying that at null, equation 1 must be modified by the addition of the small offset term

$$\Delta I = RN_o, \qquad (2)$$

where N_o is the deepest null level (the inverse of the rejection ratio, or the ratio of the system transmissions in the destructive and constructive states) which the system can attain at zero phase. Thus the fringe can be viewed as a sinusoidal fringe which is truncated at low light levels. Since this leakage term has no phase dependence, it does not affect the error signal, but it can contribute to the photon noise. The signals at the three operating points under consideration, $\phi = 0$, $\pi/2$, and π, are then RN_o, R/2, and R, respectively. For an integration time of t seconds, the respective noise levels are then $[RN_ot]^{1/2}$, $[Rt/2]^{1/2}$, and $[Rt]^{1/2}$.

For a small phase error $\Delta\phi$ about these same three operating points, the corresponding intensity changes, δI, are $R(\Delta\phi/2)^2$, $R(\Delta\phi/2)$, and $R(\Delta\phi/2)^2$, from which it can be seen that the error signals at the constructive and destructive states are indeed identical. The signal to noise ratios on the respective error signals are then $[Rt]^{1/2}(\Delta\phi/2)^2N_o^{-1/2}$, $[Rt/2]^{1/2}\Delta\phi$ and $[Rt]^{1/2}(\Delta\phi/2)^2$. In comparison to the signal to noise ratio available on the error signal at the constructive fringe, that at the destructive fringe is thus higher by $N_o^{-1/2}$, the inverse of the square root of the null ratio, due to the reduced photon noise at null. Thus, somewhat counter-intuitively, the signal-to-noise ratio on the control signal is several orders of magnitude higher at null than at the bright fringe location. Figure 6 shows an example of a dither-stabilized white light null. The sensitivity is in fact high enough that this lock was achieved with a detected photon flux at null of only 7 photons per 20 Hz dither cycle.

On the other hand, the ratio of the signal to noise available on the control signal at the quadrature

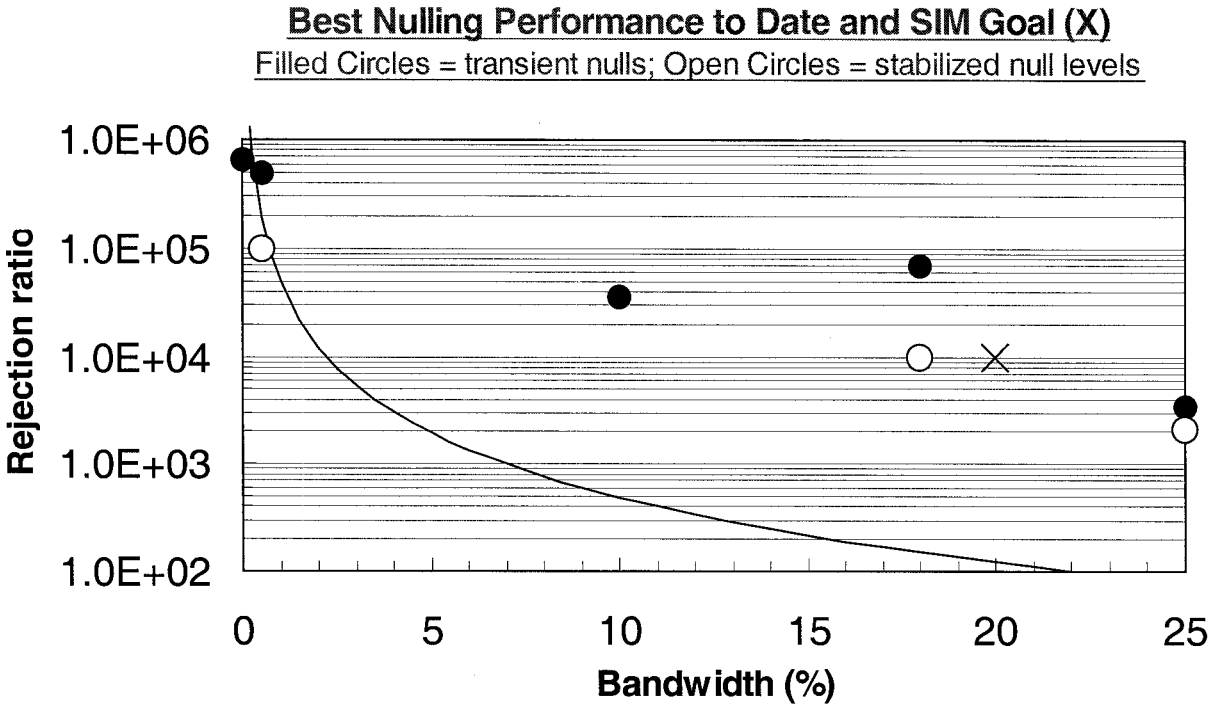

operating point to that at null is $2(2N_o)^{1/2}/\Delta\phi$. Since phase fluctuations contribute to the null level via $N \cdot N_o = (\Delta\phi/2)^2$, this ratio of signal-to-noise ratios can be rewritten $(2N_o/(N-N_o))^{1/2}$. From this it can be seen that if phase fluctuations are tiny, the quadrature operating point has large advantages, but in the more realistic case of large or dominant phase-fluctuations, only a $\sqrt{2}$ advantage is available at the quadrature point. This advantage can be amplified a bit by broadening or shifting the band sensed at the quadrature output to a (shorter) waveband where more photons are available, and by including a further factor of $\sqrt{2}$ to account for the fact that in the quadrature case the d.c. error signal is always on, while the dithered signal at null spends part of its time going through zero. Operation at the quadrature point thus brings only a relatively small increment in control sensitivity, but this may nonetheless be vital if control loop bandwidths are considered (low stellar fluxes imply small bandwidths in general). On the other hand, drifts are more of an issue for the quadrature scheme, but this can likely be overcome by periodic resets, likely a necessary calibration step in any case.

4. Summary

Laboratory experiments have been carried out at JPL to investigate both control schemes, and as Figure 7 indicates, both versions of control have successfully stabilized a nulling interferometer to deep levels (stable nulls of 10^{-4} to 10^{-5}). To date, dithering has in fact stabilized both laser and white light to the 10^{-4} level on arbitrarily long timescales, while the quadrature approach has to date only stabilized a laser, but to the 10^{-5} level. The detailed comparison of the two approaches in practise is thus not yet complete. Nontheless, a sufficient level of control has already been demonstrated to enable interesting nulling experiments both from ground-based and space-based venues.

REFERENCES

[1] K. Wallace, G. Hardy & E. Serabyn. ''Deep and stable interferometric nulling of broadband light with implications for observing planets around nearby stars,'' *Nature* ***406****, 700-702,* 2000.

[2] E. Serabyn ``Nanometer-level pathlength control scheme for nulling interferometry,'' *Applied Optics* ***38****, 4213-4216,* 1999.

[3] E. Serabyn, "Nulling Interferometry: Symmetry Requirements and Experimental Results," in *Proc. SPIE* ***4006***, ``Interferometry in Optical Astronomy'', eds. P. J. Lena & A. Quirrenbach, *328-339,* 2000.

Progress Toward Space-Based Nulling Interferometry: Comparison of Null Stabilization Approaches

IEEE Aerospace Conference
March 2001

Gene Serabyn
JPL

Nulling: Basic Concepts

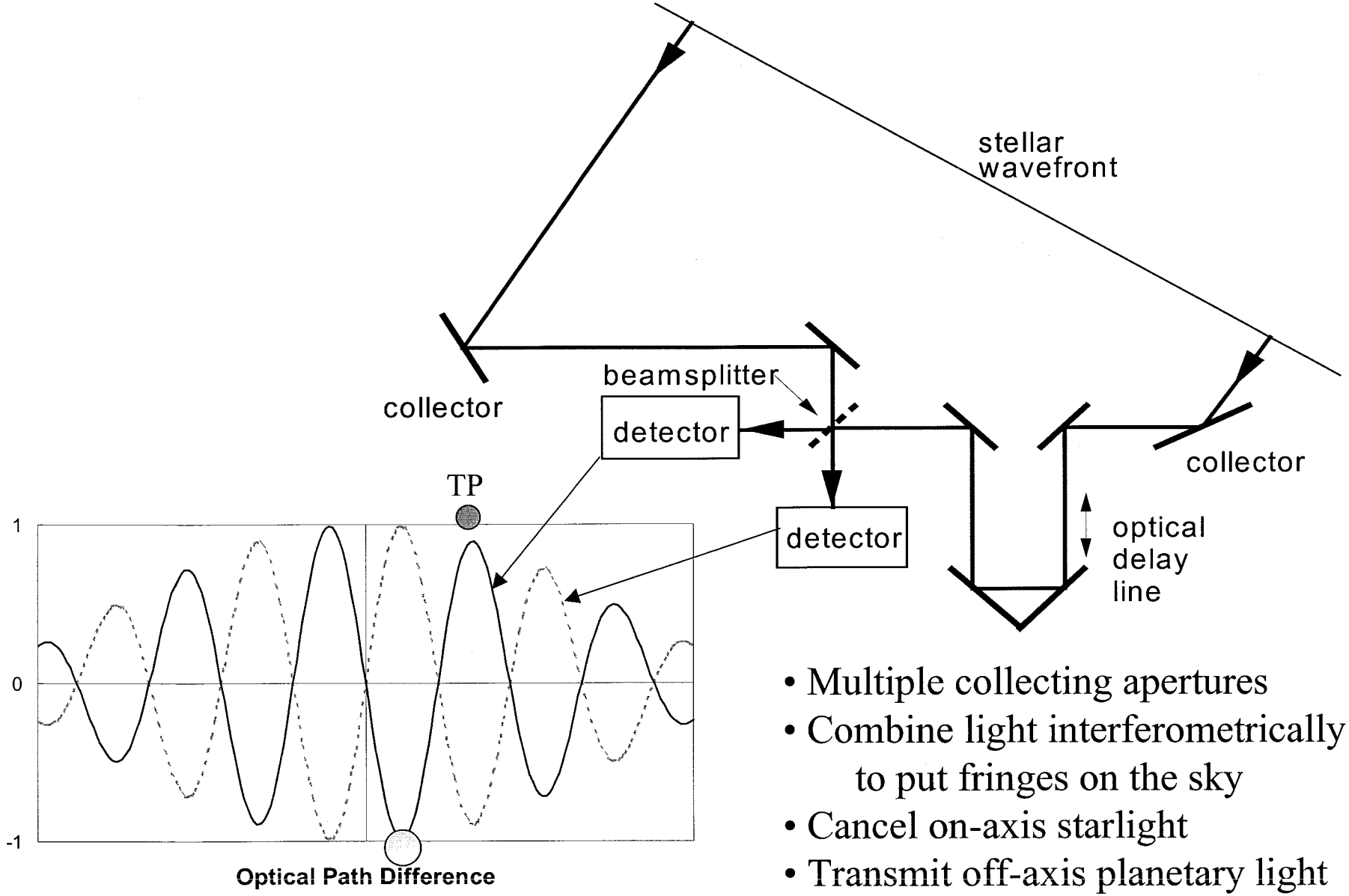

- Multiple collecting apertures
- Combine light interferometrically to put fringes on the sky
- Cancel on-axis starlight
- Transmit off-axis planetary light

How deep is your null?

- Fundamental limit: Nonzero stellar diameter limits N to:

$$N = \frac{\pi^2}{16}\left(\frac{\theta_{dia}}{\lambda / b}\right)^2$$

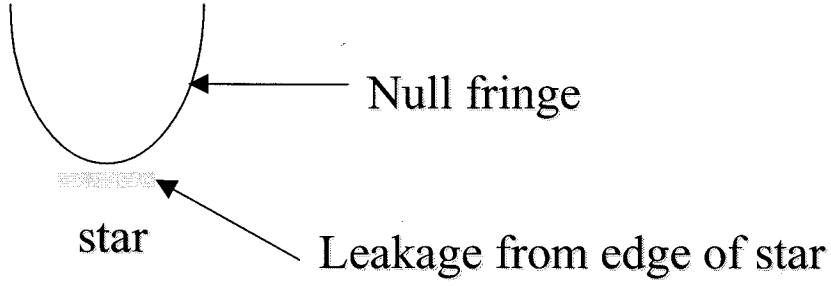

- For a G2 star @10 pc, with an angular diameter of 0.93 mas, a baseline of 85 m gives N ≈ 10^{-3} at 10 microns.

Nulling Roadmap

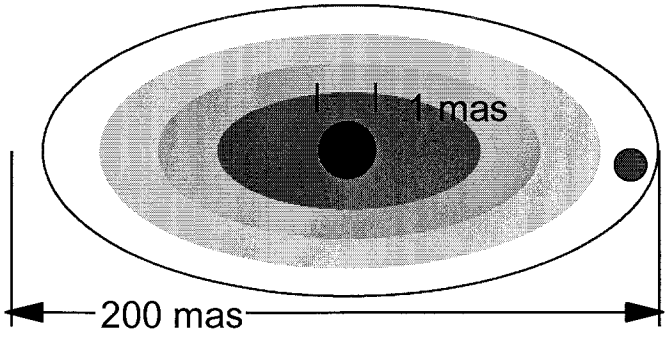

Target at 10 pc

- **Keck:** Characterize exozodiacal MIR emission around nearby stars.
  - Our 10 μm integrated zodiacal flux =
    10^{-4} of solar flux
    10^{-6} of thermal sky background

  ⇒ Null star **and** remove background.
- **SIM:** demonstrate optical nulling with nanometer-level control needed by TPF.
  - 10^{-6} null @ 10 μm ⇔ 10^{-4} null @ 1 μm

  TPF: detect planets at 10 μm in the presence of stellar, zodi, and exozodi fluxes
  - MIR (7-20 μm) null of 10^{-6}.

Original Nulling Concept

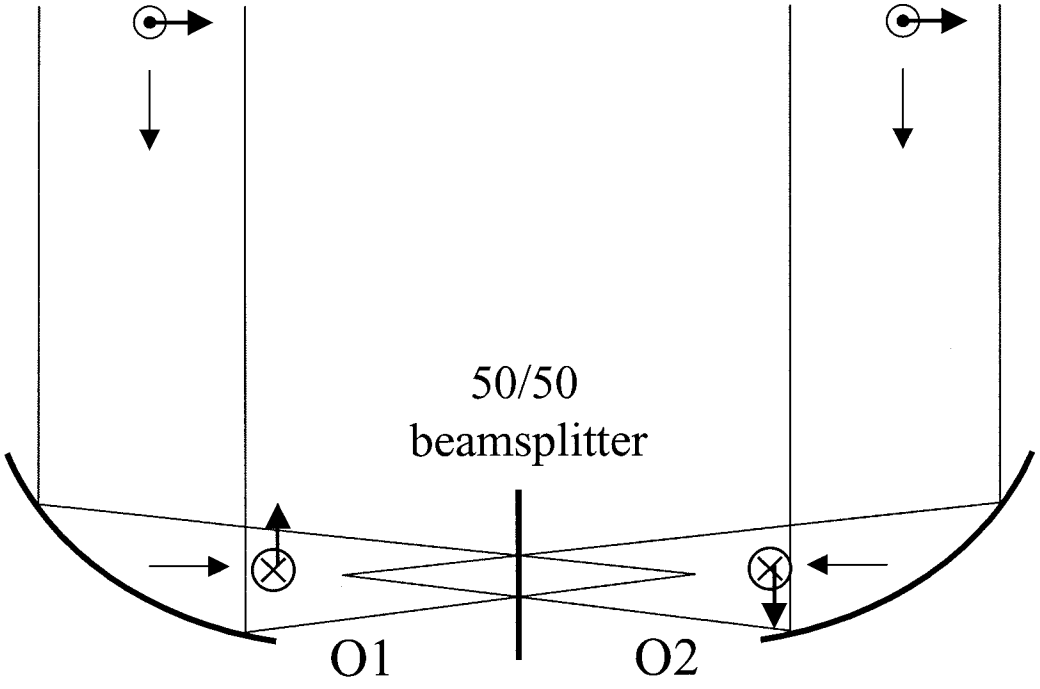

- Symmetric layout: at ZPD
  - ⇒ at ZPD equal (1/2) power to O1 & O2
  - ⇒ complementary fringes at O1 & O2
  - ⇒ no null at ZPD
- Best cancellation at finite OPD
  - ⇒ cancellation is chromatic
- 2 polarizations yield fringes out of phase by π
  - ⇒ fringe patterns cancel completely

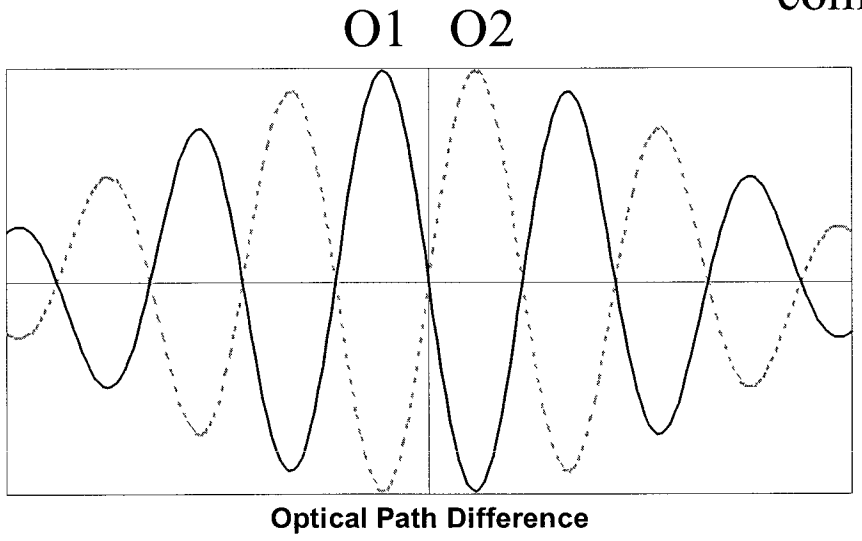

General achromatic nulling requirements

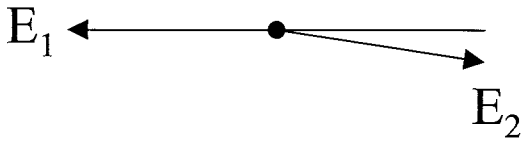

- Desire $E_1 - E_2 = 0$
- High degree of **symmetry** and **stability** required:
  - **E** fields in the two input beams oppositely oriented
  - Equal beam intensities
  - Zero relative path difference
  - Simultaneous zero of OPD for both polarizations
  - Simultaneous zero of OPD across aperture:
    Surfaces typically limit null depth to ≈ 1- Strehl ratio, or few %
    ⇒ wavefront cleanup with single mode spatial filter required
  - Simultaneous cancellation at all wavelengths in the passband
    BW evolution: SIM 20%, Keck 30 - 50%, TPF 100 %
  - Small stellar angular diameter

Achromatic Destructive Interference

- Normal ``constructive" 2-beam interferometer: $I_{out} = I_{in}(1+V\cos\varphi)/2$
- Bandwidth limitation to destructive interference minima:

$$\frac{I_{min}}{I_{max}} = \frac{1}{2}\left(1-\text{sinc}\frac{\pi}{2}\frac{\Delta\lambda}{\lambda}\right)$$

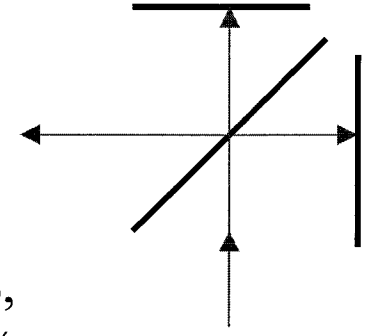

- For bandwidths of 5, 10, 20, 30, 40, and 50%,
  the deepest cancellation is 0.05, 0.2, 0.8, 1.8, 3.2, and 5%.
- Deeper cancellation requires an achromatic approach, e.g. a relative field flip:

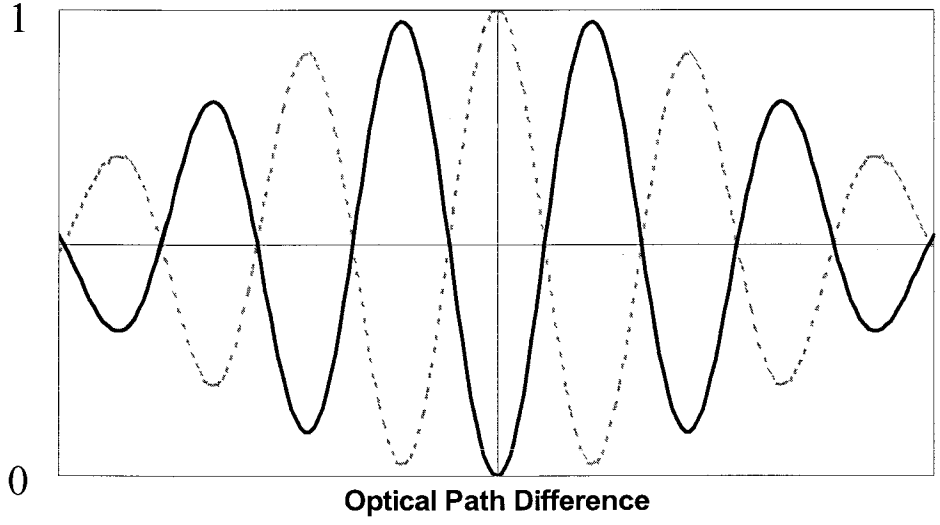

$$I_{out} = I_{in}(1-V\cos\varphi)/2$$

Electric Field Reversal

- **Achromatic field reversal can be effected by means of:**

- Geometric field flip: rotational shearing interferometer
- Through-focus field flip: (also RSI)
- Phase retardation: chromatic waveplate

Beam Combination in an RSI

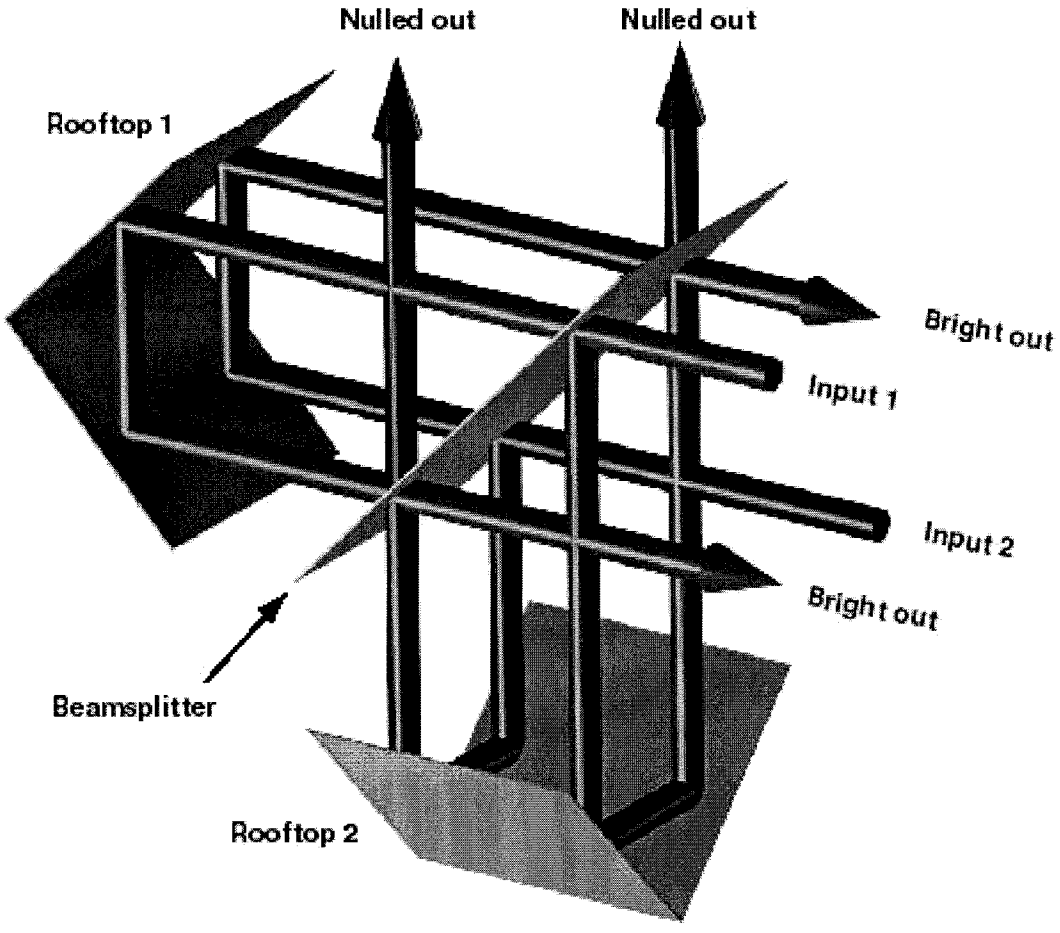

Rooftop Mirrors

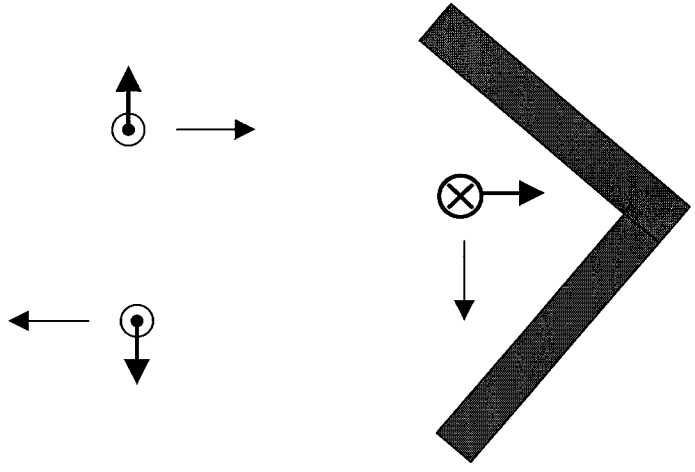

- Rooftop flips E-field component which is normal to roof line

Orthogonal Rooftop Mirrors

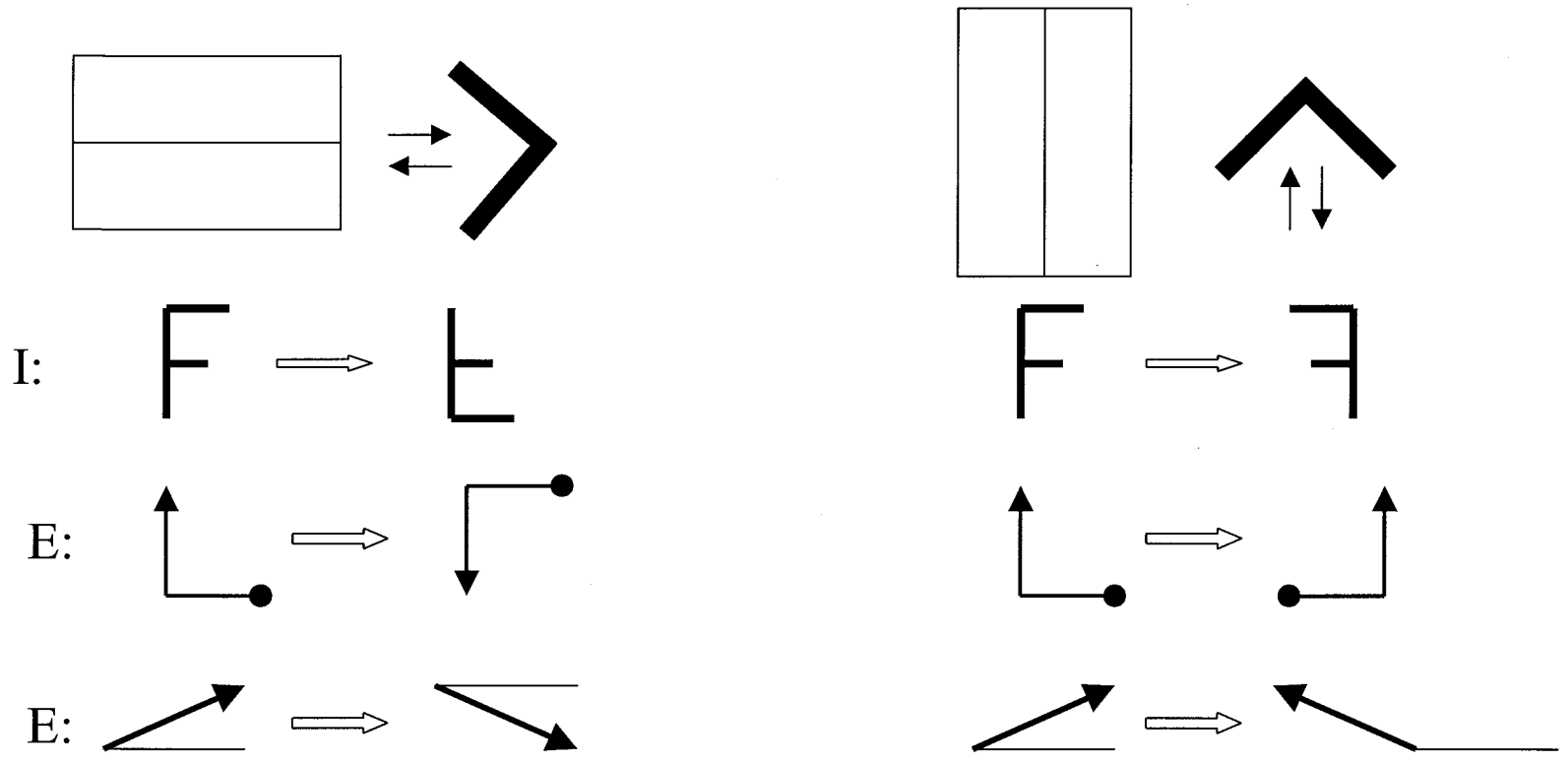

- Electric field vectors orthogonal to rooftop axis flipped by 180 degrees.
- Electric vectors parallel to rooftop axis unchanged.
- Output beams have polarizations rotated 180 degrees w.r.t. each other.
- Output apertures are rotated 180 deg. w.r.t. each other.

Single Aperture Nulling Interferometer

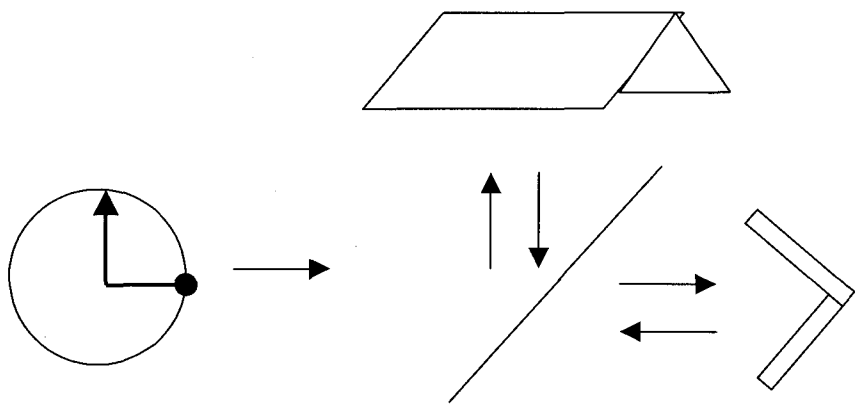

Views looking back into the beam

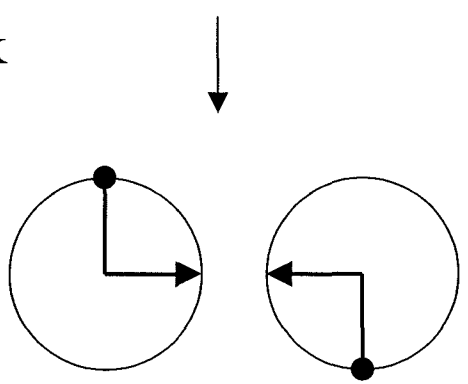

- Output images and electric fields rotated by 180 deg.
- Asymmetric: one arm has 2 s reflections, other has 2 p refl.
- Add fold mirror in each arm to symmetrize reflections:

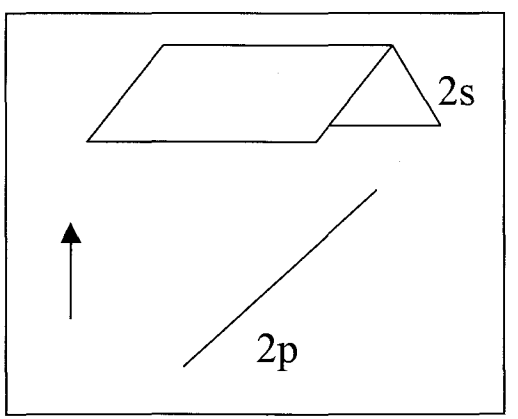

Interferometer Nuller

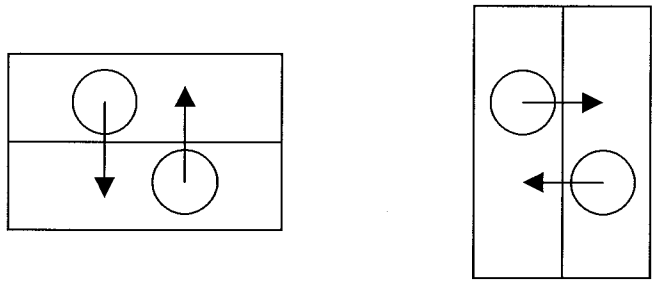

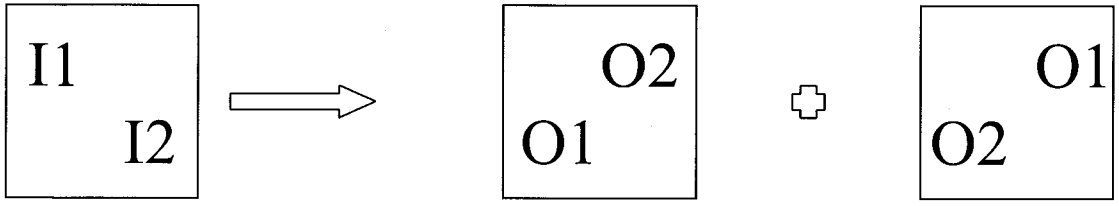

Inputs

Twin Outputs on either side of beamsplitter

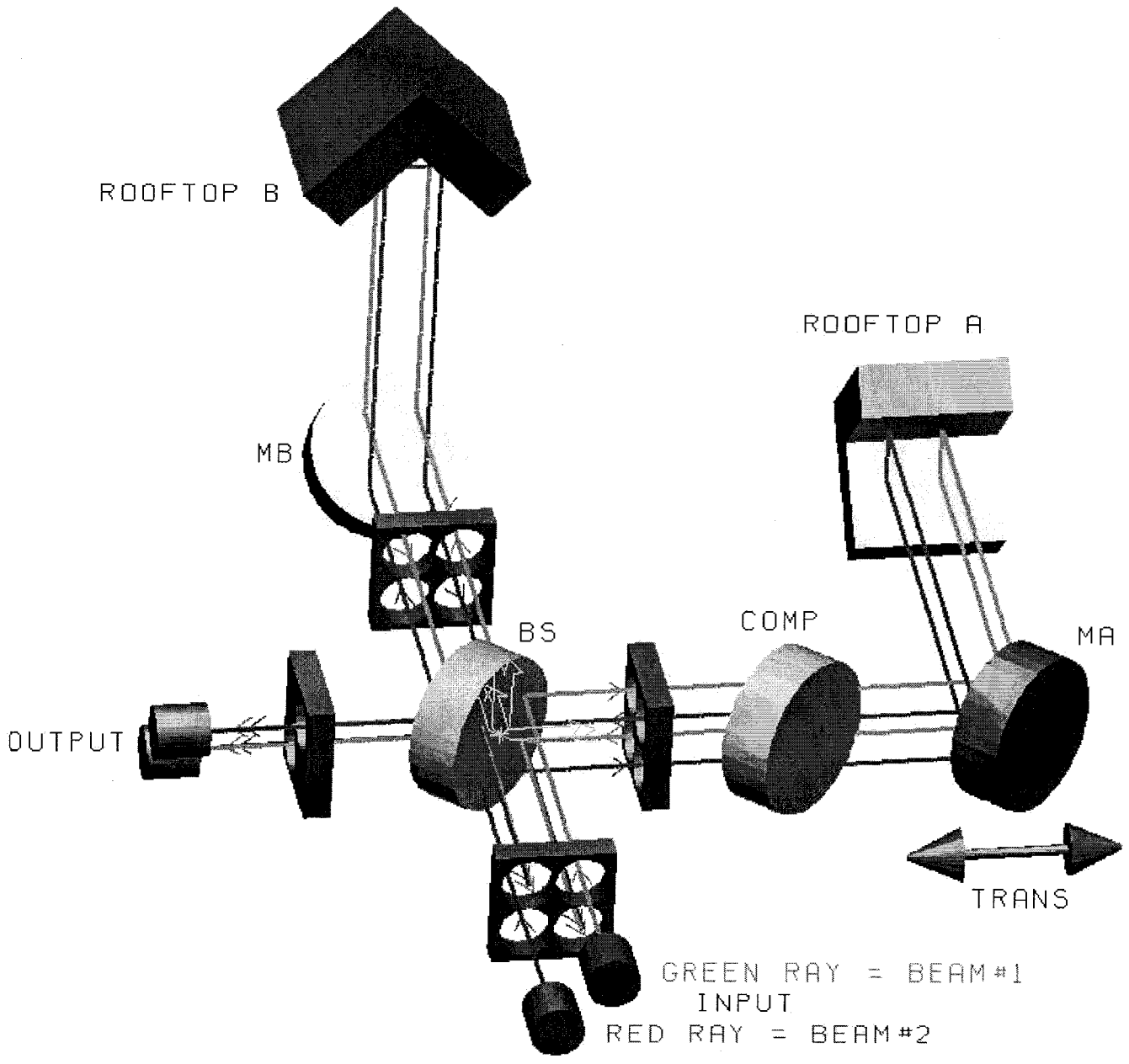
ROOFTOP B
ROOFTOP A
MB
BS
COMP
MA
OUTPUT
TRANS
GREEN RAY = BEAM#1
INPUT
RED RAY = BEAM#2

Implementation 1: rotational shearing interferometer

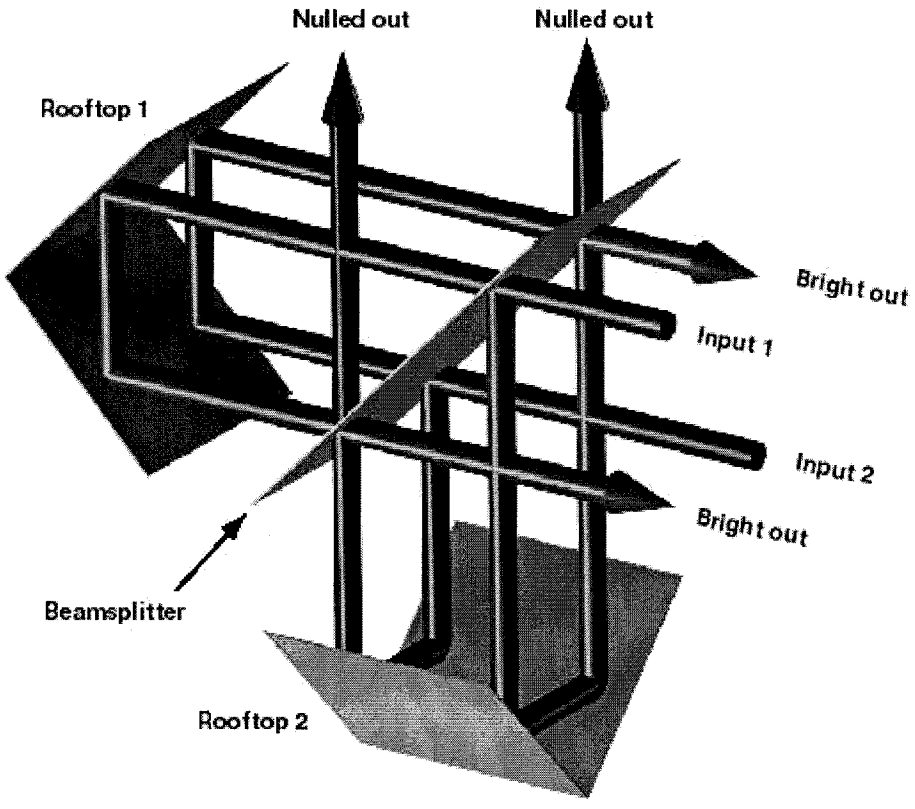

- **Advantages:**
- Relies solely on flat mirrors
- Achromatic, geometric π phase flip
- Phase flip separated from OPD
- Nearly perfect symmetry (with extra folds)
- Automatic power balance:
  Beamsplitter used in double-pass, so same RT product multiplies both inputs
- High R/T ratio tolerance at 2-pass b.s.
  (R near 0.5 only maximizes throughput)

- **Drawbacks:**
- High quality rooftop reflectors needed

- **Both:**
- 2 nulling outputs

Implementation 2: Phase shift through focus

- Passing through focus inverts aperture, adds achromatic 180 degree phase shift.
- Replace rooftops by cat's eyes:
  - one secondary flat, at focus
  - other secondary curved, prior to focus
- **Advantages:**
  - Achromatic 180 degree phase flip
  - Phase flip separated from OPD
  - Relaxed b.s. R/T requirements
- **Disadvantages:**
  - Differing angles of incidence on secs.
  - Point focus on flat secondary
  - 2 nulled outputs

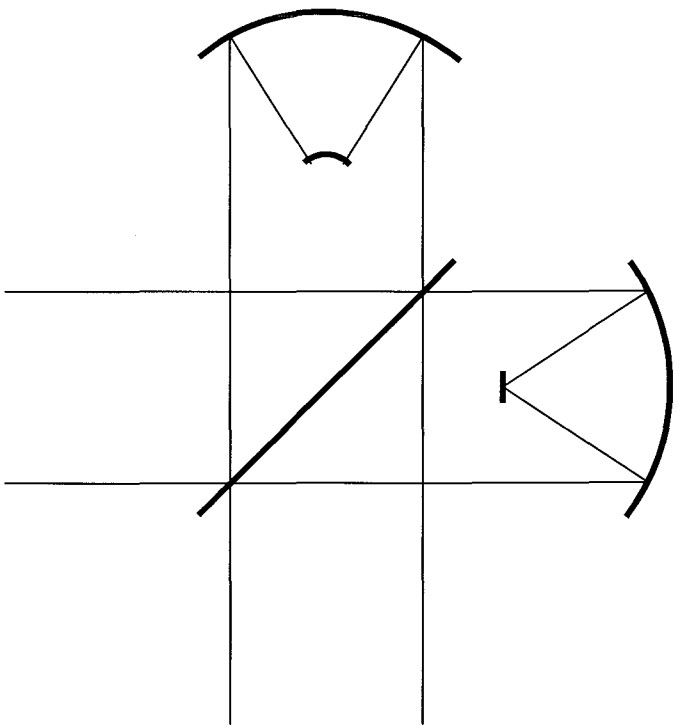

Implementation 3: dielectric waveplate

- 90 degree phase shift at b.s.
- Dielectric plate compensates for b.s. plate;
  adds another 90 degree phase shift.
- **Advantages:**
  - simple layout and components
  - no wavefront inversion
  - one nulling output
  - can use a second waveband to sense OPD
- **Challenges:**
  - Requires highly accurate coatings:
    single-pass beamsplitter requires nearly perfect R/T match for intensity balance
  - Requires highly accurate tailoring of compensator refractive indices across band.
  - Phase flip and OPD not independent.

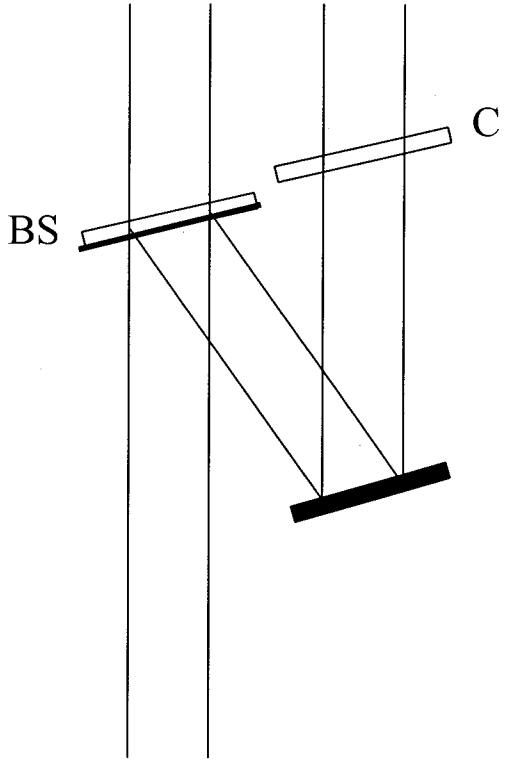

Wavefront Cleanup

- Aberrated wavefronts prohibit simultaneous field cancellation across the wavefront. N limited to about 1-S.
- Wavefront cleanup required for deep nulls
- Effected by means of a spatial filter in output focal plane
- Only the point-spread function core is transmitted
- Limits nulling to a single spatial mode of the telescope

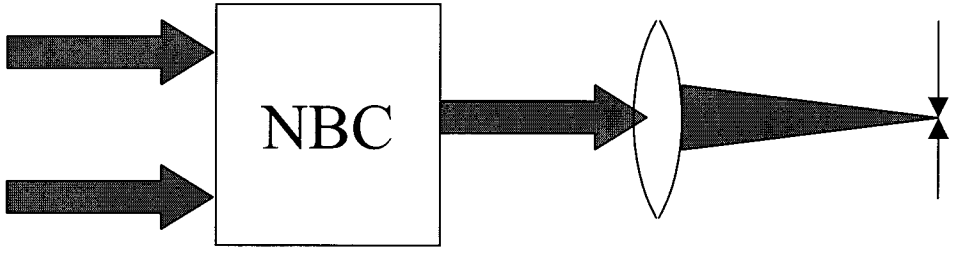

Sources of null degradation

- Finite Stellar Diameter — Static
- Nonunity visibility:
  - Wavefront errors - removed by spatial filtering — Static
  - Polarization rotation mismatch — Static
  - Intensity mismatch: transmission asymmetries, — Static
    pointing jitter induced scintillations — Fluctuating
- Nonzero phase:
  - Optical path jitter — Fluctuating
  - Differential s-p polarization delay (d1-d2 below) — Static
- Dispersion — Static

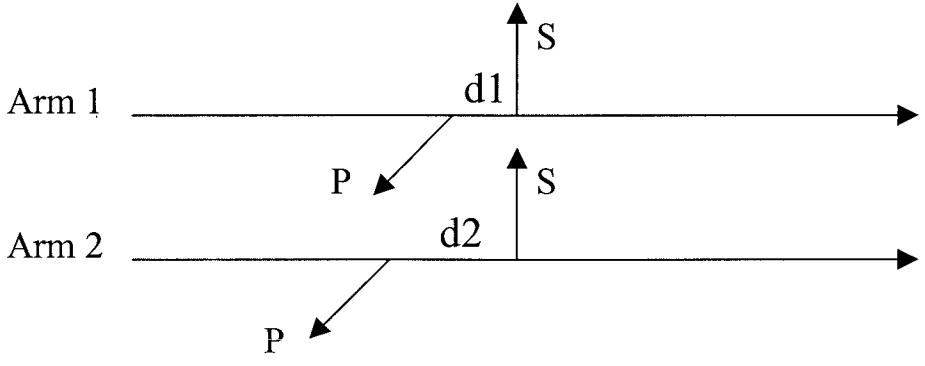

Basic Experimental Setup

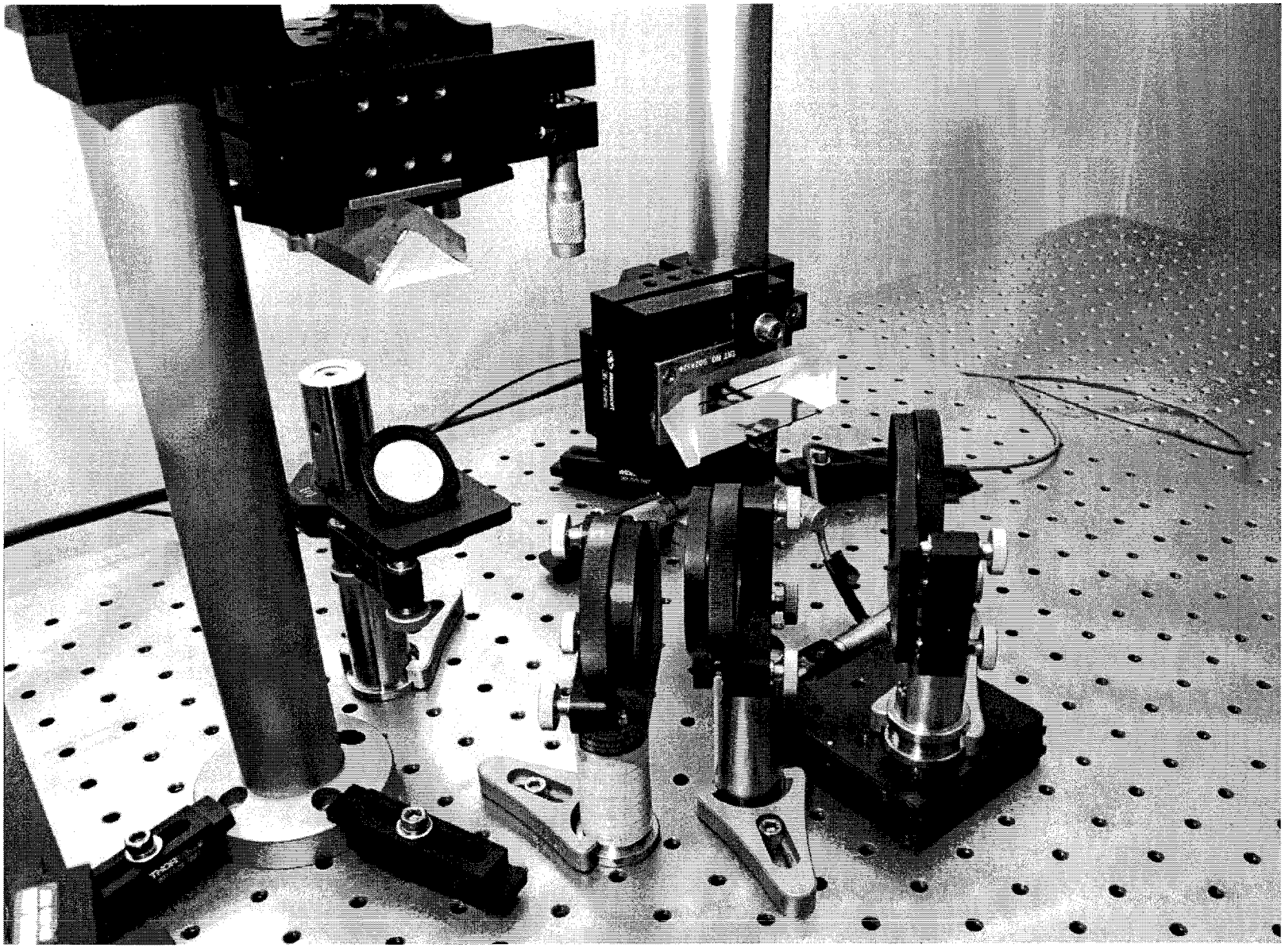

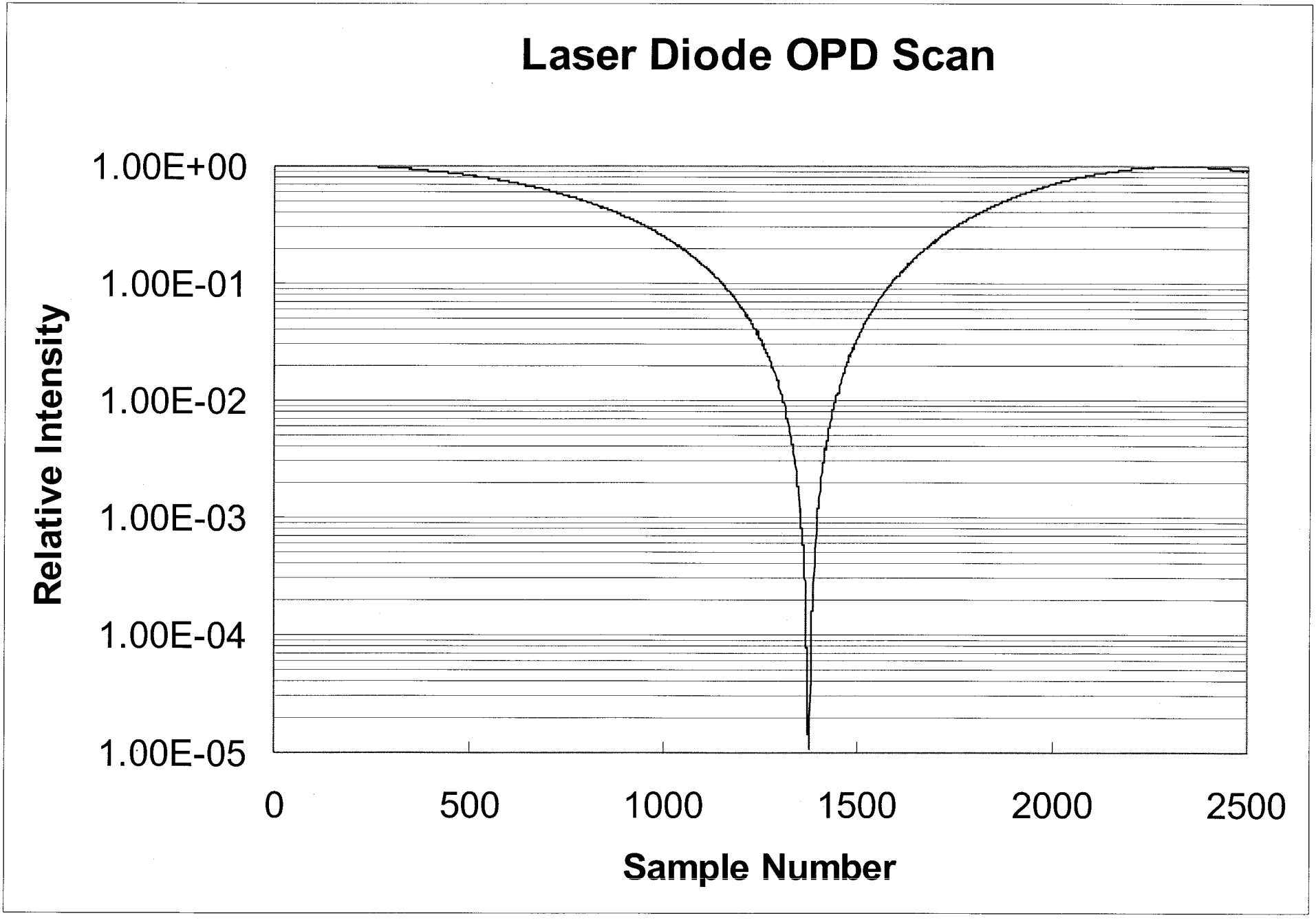
Laser Diode OPD Scan
Relative Intensity
1.00E+00
1.00E-01
1.00E-02
1.00E-03
1.00E-04
1.00E-05
0
500
1000
1500
2000
2500
Sample Number

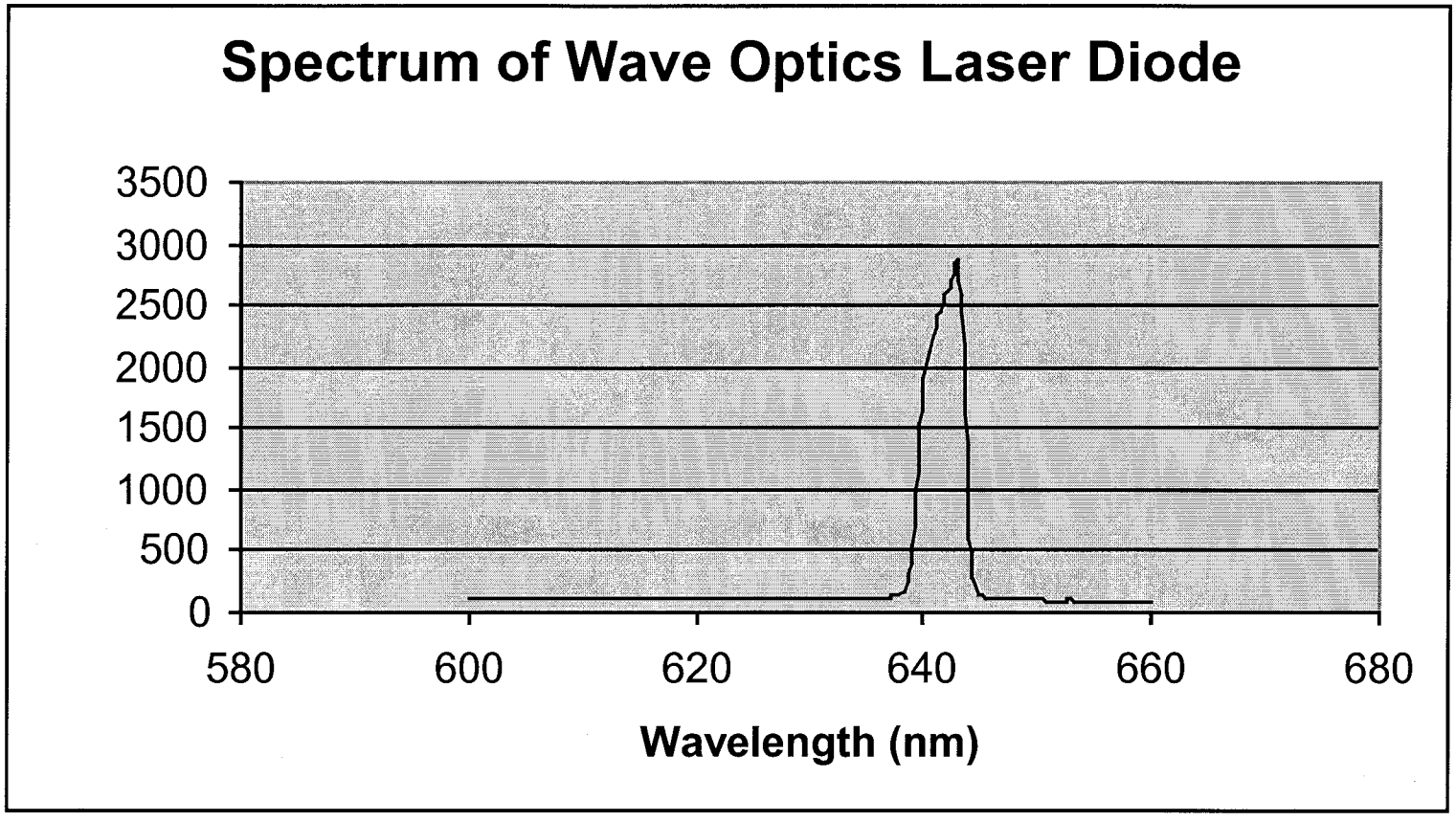

Bandwidth = 3.5 nm = 0.5%

Dither stabilization loop

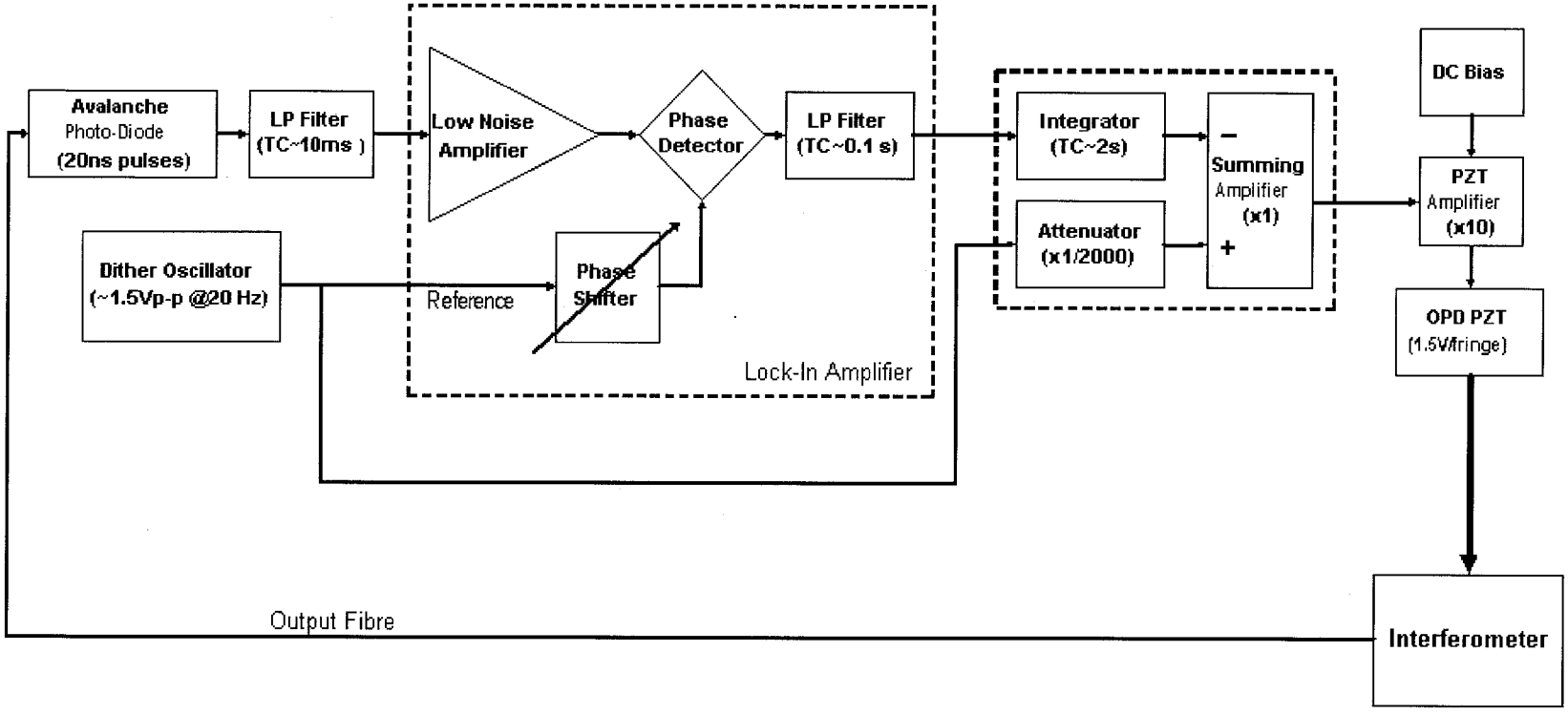

Null Stabilization Loop Block Diagram

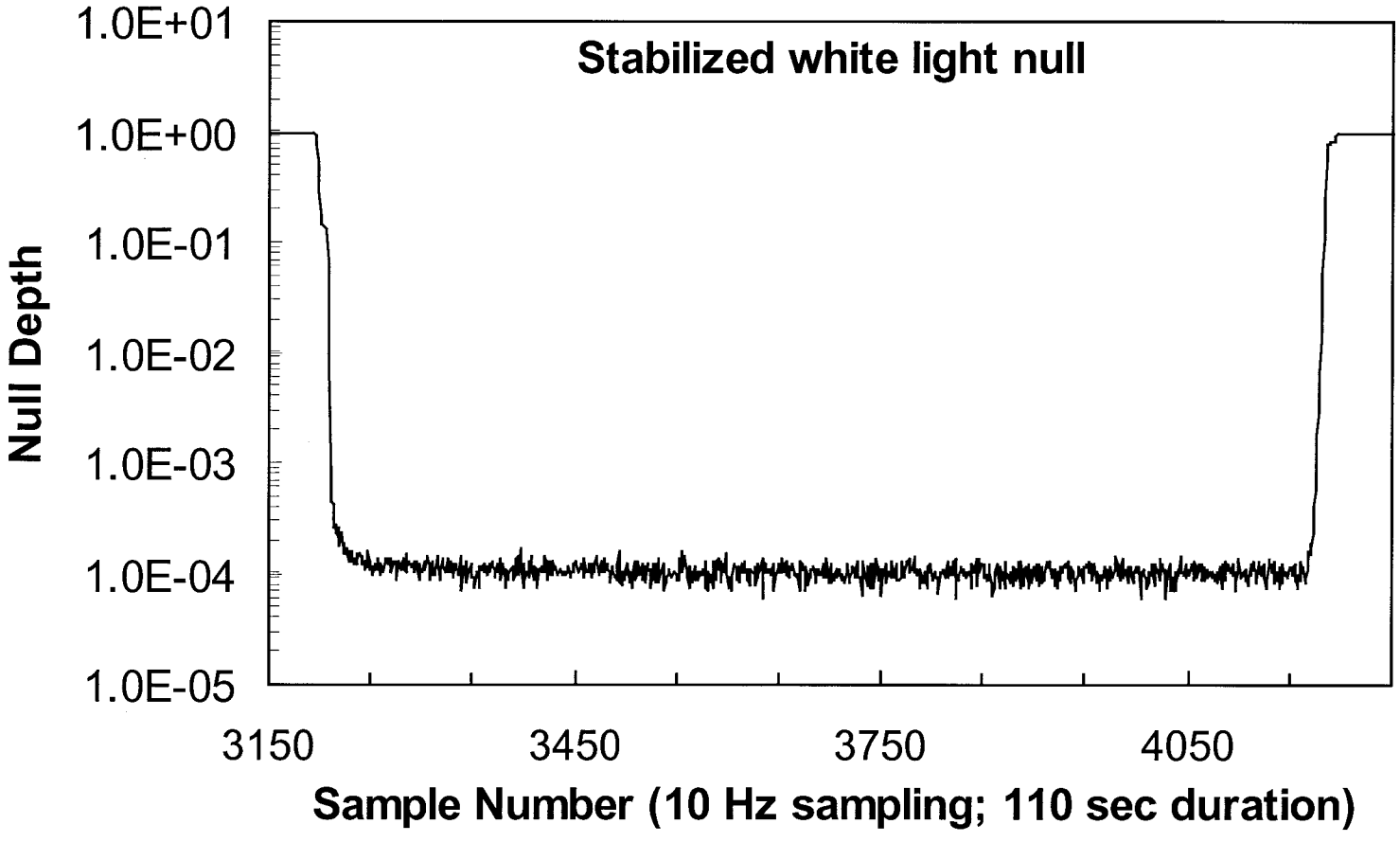
Stabilized white light null
1.0E+01
1.0E+00
1.0E-01
1.0E-02
1.0E-03
1.0E-04
1.0E-05
Null Depth
3150
3450
3750
4050
Sample Number (10 Hz sampling; 110 sec duration)

Optical OPD control

- **Approach:** The nuller has 2 outputs. Use 1 output to control the 2nd.
- **How?**

  - An *internal* nuller path delay causes the two nuller outputs to depart from null in opposite directions (opposite relative phases):

    Output 1 has E_1 ahead of E_2; output 2 has E_2 ahead of E_1.

  - An *external* path delay (i.e., prior to the nulling combiner) *always* advances one beam relative to the other.

- ∴ The 2 types of offsets can be combined to leave one nuller output on null, and the second output at an OPD offset of λ/4.
- At the quadrature output, a large signal and a linear intensity-OPD relation are available for control. Control sensitivity at half-power output:

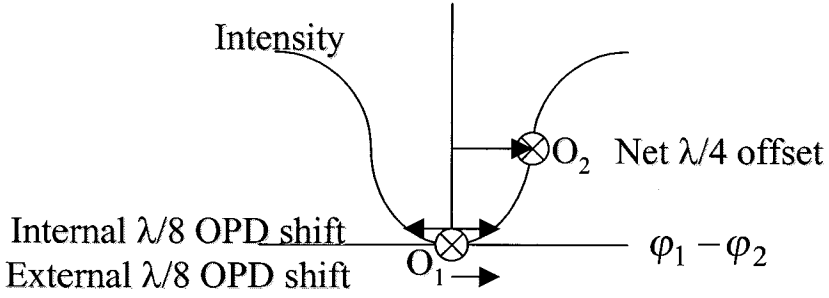

$$\frac{\Delta I}{I} = 2\pi \frac{\Delta x_{\mathrm{OPD}}}{\lambda}$$

or $\approx 1\%/\mathrm{nm}$

Two Output Experimental Setup

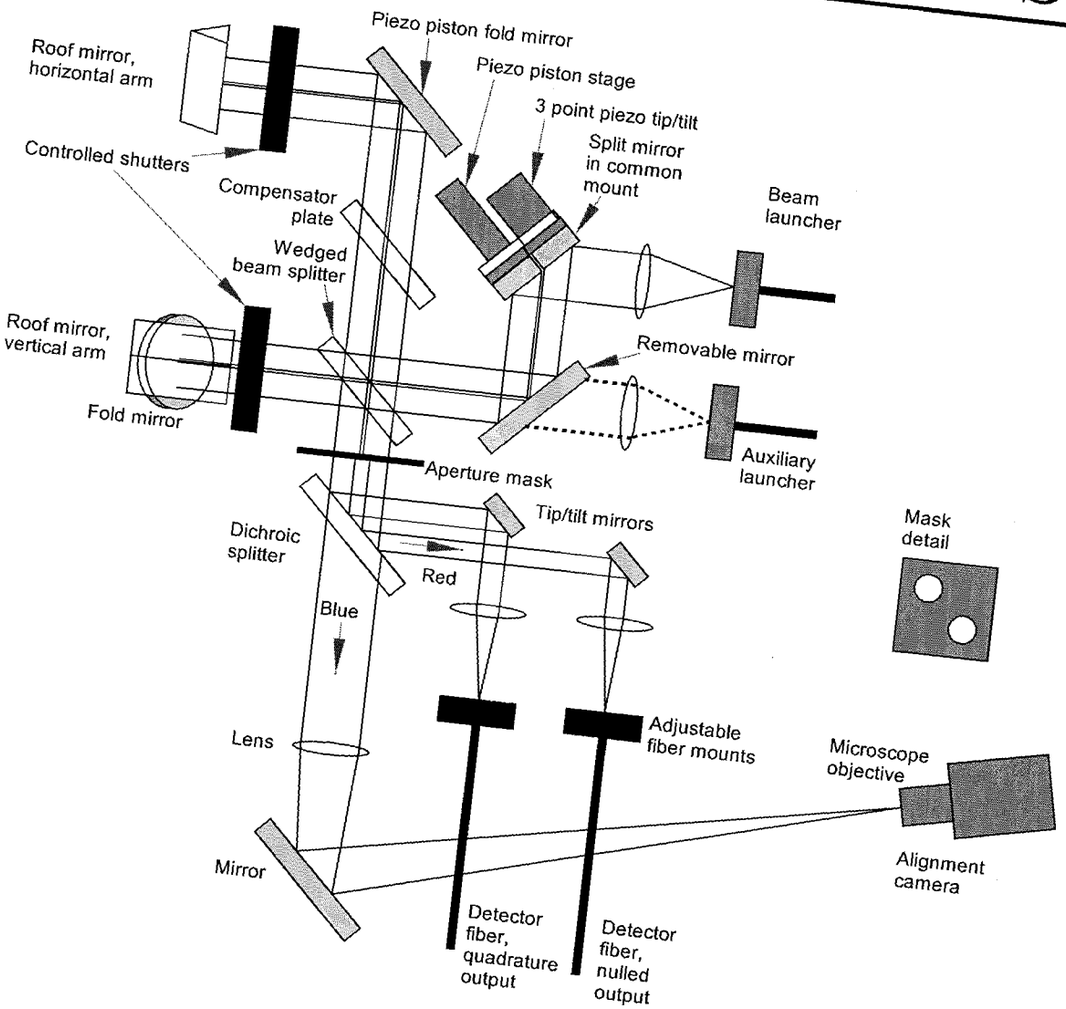

Experimental Setup

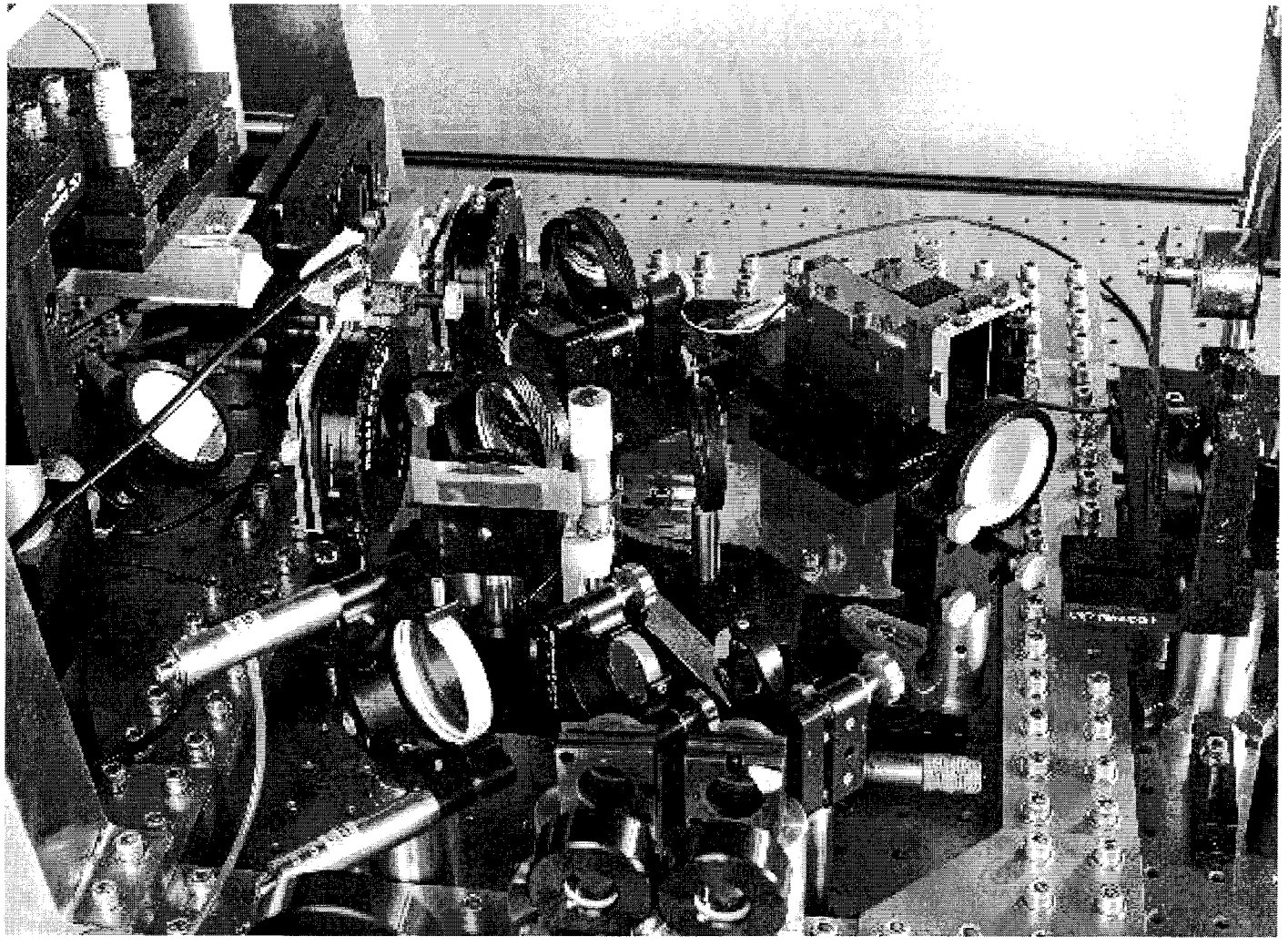

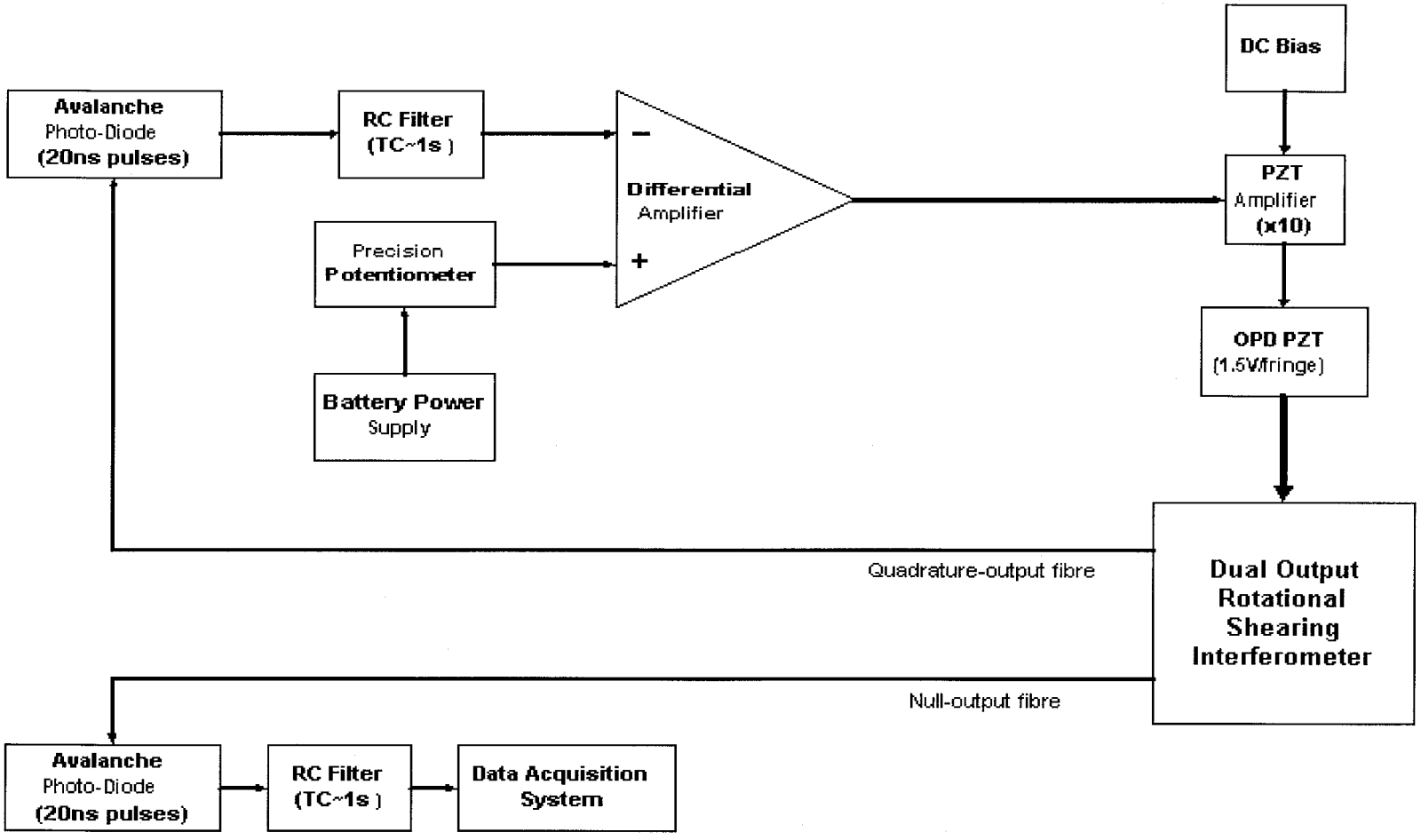

Quadrature-Output Null Stabilization Block Diagram

Quadrature-stabilized null

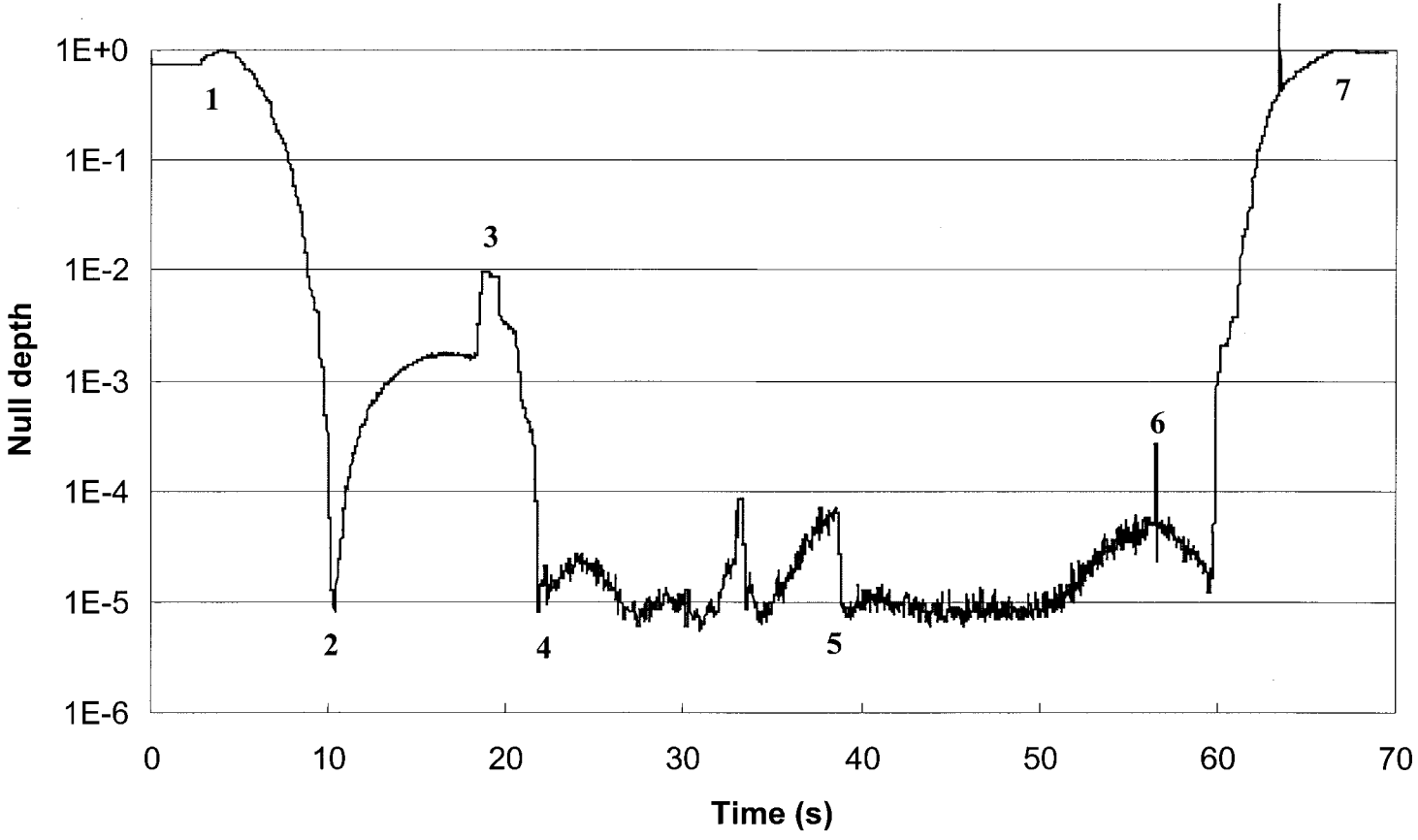

Experimental Status

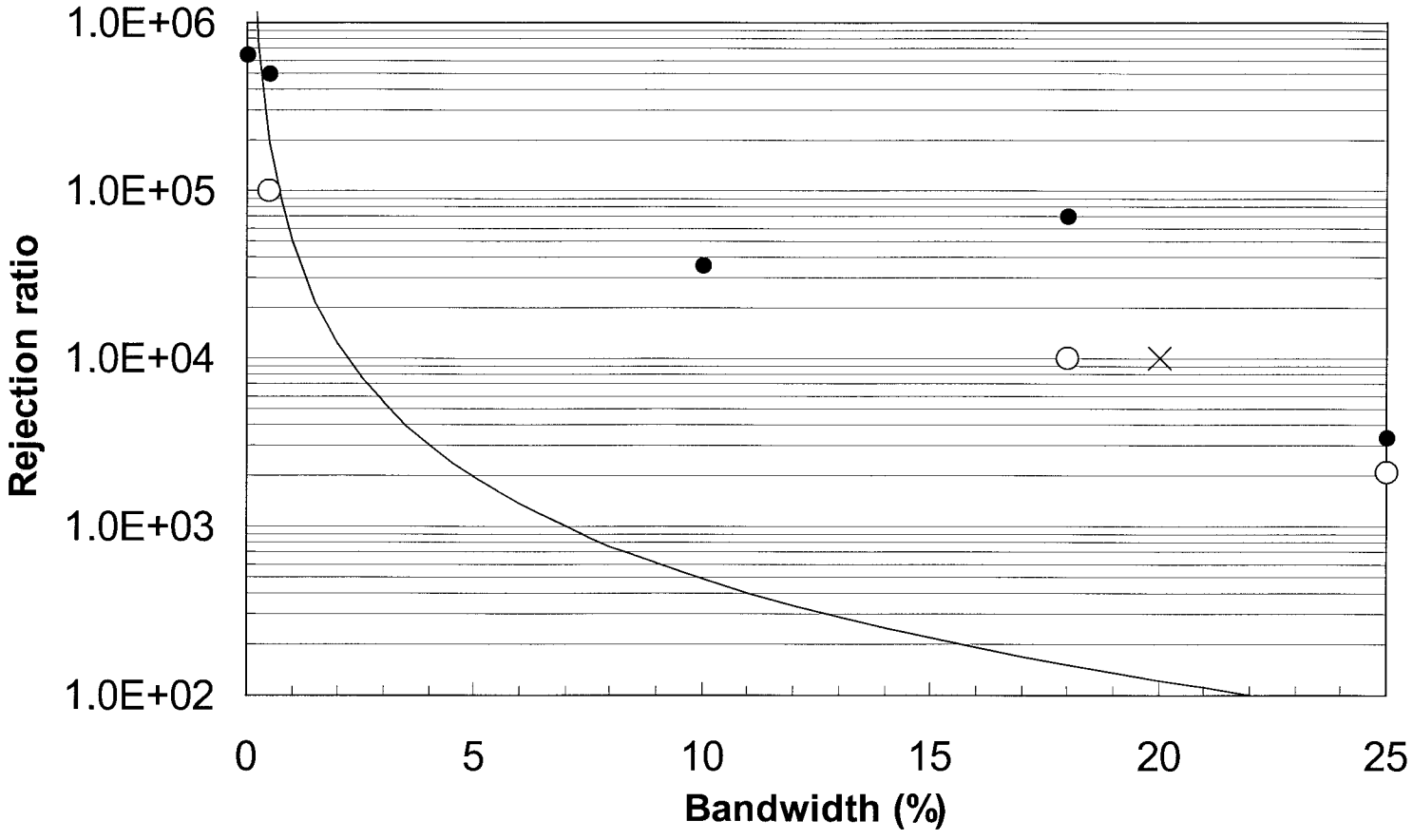

Table 1.	Null	Quadrature	Constructive
operating point phase ϕ	0	$\pi/2$	π
total flux near operating point	$R\left(N_0 + (\Delta\phi/2)^2\right)$	$R(1+\Delta\phi)/2$	$R\left(1-(\Delta\phi/2)^2\right)$
error signal	$\frac{R\delta\phi_e}{2}\cos(\omega t)$	$\frac{R\phi_e}{2}$	$\frac{-R\delta\phi_e}{2}\cos(\omega t)$
rms error signal	$\frac{R\delta\phi_e}{4}$	$\frac{R\phi_e}{2}$	$\frac{R\delta\phi_e}{4}$
error signal/ error signal near null	1	$\frac{2}{\delta}$	1
noise in time t (no background)	$\sqrt{Rt\left(N_0 + \frac{\delta^2}{8} + \frac{\overline{\phi_e^2}}{4}\right)}$	$\sqrt{\frac{Rt}{2}}$	$\sqrt{Rt}$
SNR	$\frac{\phi_e\delta\sqrt{Rt}}{4}\frac{1}{\sqrt{N_0 + \frac{\delta^2}{8} + \frac{\overline{\phi_e^2}}{4}}}$	$\phi_e\sqrt{\frac{Rt}{2}}$	$\frac{\phi_e\delta\sqrt{Rt}}{4}$
SNR/SNR_{null}	-	$\sqrt{1+\frac{2\overline{\phi_e^2}}{\delta^2}+\frac{8N_0}{\delta^2}}$	$\sqrt{\frac{\delta^2}{8}+\frac{\overline{\phi_e^2}}{4}+N_0}$
SNR/SNR_{null}	-	$\sqrt{1+\frac{\overline{N_e}+N_0}{\overline{N_d}}}$	$\sqrt{\overline{N_d}+\overline{N_e}+N_o}$
SNR/SNR_{null}	-	$\sqrt{\frac{\overline{N_{net}}}{\overline{N_d}}}$	$\sqrt{\overline{N_{net}}}$

Nifty new nuller:
Field flip by inverted right angle periscopes